

Part II

Modeling Investigation

Chapter 6

Adaptation of Existing Combustion Modeling Tools

6.1 1-D Flame Modeling using PREMIX

6.1.1 Introduction to PREMIX

PREMIX is part of the CHEMKIN family of programs, published by Sandia National Laboratories (Kee et al., 1993). PREMIX is a tool used to calculate temperatures and species profiles in a premixed flame. The calculations are limited to the dimension of flame propagation. The 1-D flame model is able to predict adiabatic flame speeds, assuming a freely propagating flame and is also able to calculate the temperature and species profiles for burner-stabilized flames. The code uses a reaction mechanism data file as input along with thermal and transport properties of the species involved in the mechanism.

The governing equations of the problem solved by PREMIX are the conservation of energy and the conservation of species. The equations are given in Equation 6.1 and Equation 6.2, respectively. The given equations allow for time variation of temperature and species profiles, but not of mass-flow. The problems solved by PREMIX are steady. A Newton algorithm is used to attempt solution from a given initial guess. The Newton algorithm operates on the steady part of the equations, i.e. the time derivative is neglected. If the Newton algorithm fails, the time derivative is added and a time integration is performed. Upon completion of a certain number of time-steps, the Newton algorithm again attempts to solve the problem. The time integration has the effect of giving the Newton algorithm a different starting point, one that may lie in the domain of convergence.

$$\rho A \frac{\partial T}{\partial t} + \dot{M} \frac{\partial T}{\partial x} - \frac{1}{c_p} \frac{\partial}{\partial x} \left(\lambda A \frac{\partial T}{\partial x} \right) + \frac{A}{c_p} \sum_{k=1}^K \rho Y_k V_k c_{p_k} \frac{\partial T}{\partial x} + \frac{A}{c_p} \sum_{k=1}^K \dot{\omega}_k h_k W_k = 0 \quad (6.1)$$

$$\rho A \frac{\partial Y_k}{\partial t} + \dot{M} \frac{\partial Y_k}{\partial x} + \frac{\partial}{\partial x} (\rho A Y_k V_k) - A \dot{\omega}_k W_k = 0 \quad (k = 1, \dots, K) \quad (6.2)$$

The freely propagating flame problem has the boundary conditions that all gradients must vanish on either end of the computational domain. The problem, with a fixed mass flow-rate, is over-determined. The mass flow-rate in this case becomes an eigenvalue that is determined as part of the solution process. For the burner-stabilized

flame, the mass flow–rate of the burner is specified along with the burner–exit gas temperature. At the downstream end of the domain all gradients again vanish. The upstream boundary conditions specify the species composition of the mixture along with the gas temperature. The result is that for burner–stabilized flames, heat will be conducted out of the computational domain. The heat–loss lowers the flame–speed to match the incoming mass flow–rate.

For greater detail about the algorithms used, the discretization employed and other computational aspects of PREMIX, the reader is referred to the Sandia Report referenced (Kee et al., 1993).

6.1.2 Modifications to PREMIX

The PREMIX Fortran source code was modified to accomplish two major improvements. First, the program was changed to allow for better computational resolution and easier post–processing. Better computational resolution was achieved by allowing the user to specify the maximum number of points allowed in the computational model. The original version of PREMIX had a maximum point number of 69. Solutions discussed in the present report at times use greater than 500 points. Easier post–processing was implemented by writing a separate output file, specifically designed for import into a spreadsheet.

The second major improvement was to change the program so that axial flame heat–loss may be accounted for in the model. The heat–loss may either be convective or radiative. The heat–loss term is added to the energy equation given in Equation 6.1. The modified expression is given in Equation 6.3.

$$\rho A \frac{\partial T}{\partial t} + \dot{M} \frac{\partial T}{\partial x} - \frac{1}{c_p} \frac{\partial}{\partial x} \left(\lambda A \frac{\partial T}{\partial x} \right) + \frac{A}{c_p} \sum_{k=1}^K \rho Y_k V_k c_{pk} \frac{\partial T}{\partial x} + \frac{A}{c_p} \sum_{k=1}^K \dot{\omega}_k h_k W_k + \frac{Q'_{loss}}{c_p} = 0 \quad (6.3)$$

Some other modifications include a feature to make the program more stable and prevent frequent program restarting. None of the above modifications prevent any previously existing features from being used. The program was further modified for modeling the honeycomb burner as described in Chapter 8. Further description of

the code modifications and the list of newly defined keywords for use in PREMIX input files can be found in Appendix B.

6.2 Chemical Kinetics Modeling

6.2.1 Reaction Rate Modeling

To model a reaction such as that given for CH* formation given in Equation 1.4, the reaction rate must be quantitatively determined. For a reaction of n moles of A with m moles of B, the forward reaction rate is given by the form given in Equation 6.4 using the modified Arrhenius expression for the reaction rate constant.

$$k_f = [A]^n [B]^m A T^\beta e^{\frac{E_a}{R_u T}} \quad (6.4)$$

The reaction rate parameters are thus A, β and E_a . If the given reaction is reversible, the equilibrium constant for the reaction determines the rate constant of the reverse reaction. The equilibrium constant is only a function of temperature. Once the forward and reverse reaction rates are calculated, the net destruction and generation of species can be calculated along with the associated energy exchange. Equation 6.4 also shows the highly non-linear coupling between the species equation and the energy equation. The reaction rate has an exponential dependence on temperature.

6.2.2 Introduction to GRIMECH 3.0

GRIMECH 3.0 (Smith et al., 1999) is the third edition of a system of reactions that models the combustion of methane. GRIMECH is packaged to be processed by the PREMIX pre-processor program CKINTERP which generates a binary file to be used as PREMIX input. The reaction mechanism consists of more than 250 reactions. Formation of nitrogen oxides is included in the model. The individual reaction rate parameters are taken from a variety of sources.

Once compiled, the reaction mechanism is optimized using global experimental observables, such as adiabatic flame speed as calibration standards. Most of the reactions in the mechanism are however not optimized since the experimental observables

generally used are only sensitive to very few of the more than 250 reactions. The result is that the reaction mechanism contains many reactions that have rate constants with large uncertainties.

6.2.3 Modifications and adjustments in GRIMECH 3.0

A detail listing of the reaction mechanism used in the present studies is given in Appendix A. The reaction mechanism as published, includes nitrogen oxide chemical reactions. These reactions are taken out of the mechanism because the reactions have a negligible effect on temperature and other species concentrations. Furthermore, nitrogen oxide formation is not part of the present study. The chemiluminescent species formation equations are not included in the published reaction mechanism and needed to be added.

OH* reactions

Two different OH* formation reactions are used in two separate versions of the mechanism. Both versions are used in the honeycomb modeling calculations (see Section 8.4) for comparison to experimental data (see Section 5.2). The first version of the mechanism uses the traditionally accepted reaction given in Equation 1.1 with the accepted reaction rate constant of 1×10^{-13} cc/(molecule-sec). The second reaction has not been discussed in the literature but is postulated to describe the correct formation path of OH*. The reaction is given in Equation 6.5. The rate constant for the reaction given in Equation 6.5 is calculated as part of a chemiluminescence modeling optimization process discussed below.



To begin to justify Equation 6.5 as the formation path for OH*, consider the reaction of CH and molecular oxygen as it is treated in literature. In some reaction mechanisms the reaction between CH and molecular oxygen goes directly to carbon monoxide and an unexcited hydroxyl radical (Frenklach et al., 1992). GRIMECH does not have that reaction, instead GRIMECH has a reaction from CH and molecular oxygen to

HCO and O and then another reaction that takes HCO and O and produces carbon monoxide and an unexcited hydroxyl radical. Overall, the two models are identical and the first mechanism (Frenklach et al., 1992) merely represents a simplification of the second reaction mechanism. The formation path for OH* given in Equation 6.5 suggests that the original path given in Equation 1.1 is an over-simplification. Much more detailed justification for using Equation 6.5 as the OH* formation path is given in Section 9.1.

The quenching reactions for OH* are taken directly from Dandy and Vosen (1992) for both formation paths. All reactions involving OH* are irreversible.

The properties for OH* are taken to be identical to those of the unexcited hydroxyl radical with the exception of the heat of formation which is increased, as suggested for CH* by Frenklach (1992).

The rate of radiant transition of OH* to unexcited OH has a theoretically calculated value given by the Einstein coefficient. For OH* the coefficient has a value of 1.7×10^6 1/sec.

CH* reactions

The CH* formation reaction is adopted exactly as given by Equation 1.4 (Devriendt and Peeters, 1997) with a reaction rate constant of $4.187 \times 10^{12} e^{-\frac{230}{T}}$ cc/(mole-sec). The problem for CH* is obtaining reliable, detailed quenching data. The most recent data on CH* quenching has been compiled by Garland and Crosely (1986). As alluded to in Section 1.3.2, the OH* quenching model was found to successfully reproduce quenching data whereas the CH* quenching model was not able to do the same. Garland and Crosely suggested that CH* quenching is extremely temperature sensitive, even more so than OH*. The development of the quenching model described in the next paragraphs uses the data compiled by Garland and Crosley as guidance.

The radiant transition rate coefficient, the Einstein coefficient has a value of 1.9×10^6 1/sec for CH* transition to unexcited CH.

As with OH* chemical kinetics, all CH* reactions are irreversible. The properties for CH* are identical to those of CH with the exception of the heat of formation which

Table 6.1: Comparison of chemiluminescence quenching models

Quenching Molecule	CH* Quenching		OH* Quenching	
	Rate Coefficient	Temperature Exponent	Rate Coefficient	Temperature Exponent
O ₂	1.929x10 ¹²	0.75	9.5x10 ¹⁸	-0.4
H ₂	1.866x10 ¹⁰	1.773	5.6x10 ¹⁸	-0.55
N ₂	2.722x10 ¹²	0.6	5.6x10 ¹⁸	-0.35
H ₂ O	9.232x10 ¹¹	1.1	2.7x10 ¹⁹	-0.35
CH ₄	3.653x10 ¹⁰	1.773	4.9x10 ¹⁸	-0.2
CO	7.794x10 ¹²	0.714	2.4x10 ¹⁹	-0.47
CO ₂	1.143x10 ¹¹	1.1	5.1x10 ¹⁹	-0.56
C ₂ H ₂	3.166x10 ¹²	1.1	—	—
C ₂ H ₆	1.925x10 ¹¹	1.773	—	—

is increased as suggested by Frenklach (1992).

Chemiluminescence model optimization

Several parameters in the chemiluminescence model still need to be fixed to complete the reaction mechanism. The reaction rate coefficient for the OH* formation reaction given in Equation 6.5 must be determined and the quenching model for CH* must be developed. The details of how the chemiluminescence model was completed are given in Section 6.2.4. The result of the analysis for the reaction rate coefficient of Equation 6.5 is a value of $4.8 \times 10^{-11} e^{-\frac{230}{T}}$ (cc/molecule-sec). The detail results of the quenching model for CH*, in comparison to OH* may be viewed in Table 6.1.

6.2.4 Chemiluminescence model completion

The process of completing the chemiluminescence is complicated by the fact that neither chemiluminescent species reaction mechanism is completely known. Based on the experimental results, it is difficult to defend Equation 1.1 for OH* formation, but Equation 6.5 is completely unknown. The experimental results do seem

to show several relationships among chemiluminescence results that remain invariant for changes in operating condition and thus may be used in attempting to fix the uncertain parameters of the chemiluminescence model. Before explaining in detail how the chemiluminescence model is completed, several analysis tools which are used in the process are introduced.

PREMIX results processing

PREMIX results include complete species and temperature profiles through the flame. To obtain the total chemiluminescence from the profiles, Equation 6.6 was programmed in both the post-processing routine inside PREMIX as well as externally as a spreadsheet macro.

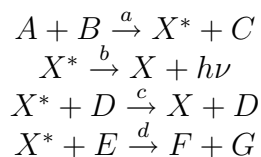
$$X_{tot}^* = \int_{x_{start}}^{x_{end}} A_{Einstein} [X^*]_{local}(x) dx \quad (6.6)$$

The integral given in Equation 6.6 is calculated using the simple trapezoidal rule because of the uneven grid spacing. Since the equations solved by PREMIX, and thus the results are based on a flow that is specified in mass-flow per unit area, the resulting chemiluminescence yield calculated by Equation 6.6 must also be interpreted as being on a per unit area basis, i.e. the quantity calculated has the units of light intensity.

Simplified chemiluminescence analysis

Even without considering the chemiluminescence species output, PREMIX 1-D flame calculations provide complete profiles of all the species participating in chemiluminescence formation. These profiles provide the key to efficiently completing and iterating on the chemiluminescence model. The profiles of the participating species through the flame are used for the complete calculation of the chemiluminescence species profiles for varying quenching and reaction rate parameters, under the assumption that chemiluminescence formation and destruction does not significantly affect the precursor or product species concentration variation through the flame.

Table 6.2: Example chemiluminescence mechanism



The assumption is verified at the end of the analysis by performing a full mechanism calculation.

A further assumption required to calculate the variation of chemiluminescence species concentrations through the flame is the assumption that the chemiluminescence species, may be subjected to the assumption of the steady state of intermediates (SSI). SSI, a classic chemical kinetics analysis tool, has the mathematical representation given in Equation 6.7. The SSI assumption is applicable whenever a minor species is destroyed much more quickly than the species is produced (Turns, 1998). Equation 6.7 forces a balance between production and destruction of the species in question.

$$\frac{d [X^*]}{d t} = 0 \tag{6.7}$$

To illustrate how the SSI assumption is used to calculate the chemiluminescence species concentration from the given precursor concentrations, consider the simple, representative reaction mechanism shown in Table 6.2. In the example mechanism, the first reaction with rate constant *a*, represents a typical chemiluminescence species production reaction. The second reaction with rate constant *b*, represents the radiant transition to the stable molecule. The third reaction with rate constant *c*, represents the destruction of the chemiluminescent molecule by a non-reactive collision. The last reaction with rate constant *d* represents the destruction of the chemiluminescent molecule by a reactive collision.

In the example chemiluminescence mechanism, the concentrations of the molecules A, B, D and E are all known. The balance equation, Equation 6.7 can now be used to

obtain an expression for the concentration of the chemiluminescence species. For the example mechanism of Table 6.2, the solution is given in Equation 6.8. The chemiluminescence yield is then obtained by calculating the rate of reaction two, since the rate of this reaction determines the rate of production of radiation $h\nu$.

$$[X^*] = \frac{a [A] [B]}{b + c [D] + d [E]} \quad (6.8)$$

Chemiluminescence model parameters

The parameters available for model optimization are the rate parameters of Equation 6.4. For quenching reactions, the activation energy, E_a is generally set to zero. The parameters that remain for quenching reactions are k_a , the forward rate coefficient and β , the temperature exponent for the rate expression. For the chemiluminescence formation equation given in Equation 6.5, the activation energy, E_a is set to the same value as that for the CH^* production equation since the reactions are similar in that they both involve an oxygen atom as well as a three-atom unstable radical. The temperature exponent, β again analogous to the CH^* production reaction is set to zero. The only remaining parameter to be set is then the forward rate coefficient, k_a .

Chemiluminescence model optimization process and results

The optimization is centered around experimental and analytical data for three equivalence ratios: 0.80, 1.00 and 1.10. To evaluate a certain CH^* quenching parameter setting with respect to experimental data, the relative increase or decrease of mass-flow specific chemiluminescence yield from an equivalence ratio of 0.80 to 1.00 and from 1.00 to 1.10 is used.

The quenching molecules considered in the CH^* quenching model include the same molecules considered for OH^* quenching. The complete list of quenching molecules considered is given in Table 6.1. It was found that both the rate coefficient and temperature dependence of the following quenching molecules needed to be raised significantly: H_2 , CH_4 , CO_2 , C_2H_2 and C_2H_6 . In the course of the optimization process, the

production of the precursor to CH^* , C_2H was also scrutinized and some reaction rate parameters were changed in the production and consumption path of C_2H as well.

The changes in the reaction rate coefficients are in all cases inside the uncertainty of the given reaction rate parameters. To determine the uncertainty, the origin of the reaction was investigated on the GRIMECH 3.0 web-site (Smith et al., 1999) and compared to other references such as Frenklach (1992) or Turns (1996). The optimization process thus also required a change in the calculated reaction rate given by Devriendt (1997). The reaction rate given was reduced by two thirds. The reduction was applied to all C_2H consumption reactions involving the oxygen atom or molecule. The consumption reactions rates of C_2H involving the hydrogen atom or molecule were increased by 250%. The C_2H production reaction rate temperature dependencies were increased, keeping the overall reaction rate constant at a temperature of 1700 °K. The C_2H_2 consumption reactions were all adjusted to maintain the same branching ratio for each of the consumption paths as prior to the modification. Finally, the association reaction rates of two methyl molecules were lowered by 33%.

All of the changes undertaken in the model attempt to decrease the production of CH^* chemiluminescence at higher equivalence ratios. The quenching efficiencies of carbon and hydrogen containing molecules were increased and consumption of C_2H by hydrogen type molecules was encouraged. All these changes managed to lower the ratio of CH^* radiation from an equivalence ratio of 0.80 to 1.10 from approximately 25 to approximately 12. The experimental data showed a ratio of approximately 8. The model could be forced to match the experimental data but the quenching data that exists (Garland, 1986) would then be ruthlessly contradicted. It is important that although many changes to the quenching model and C_2H production have been implemented, no existing experimental data is contradicted.

The production reaction rate of OH^* through Equation 6.5 is set by matching experimental and analytical OH^* to CH^* chemiluminescence emission intensity or rate ratios at an equivalence ratio of 0.90.

6.3 FLUENT Computational Fluid Dynamics

FLUENT is a powerful computational fluid dynamics (CFD) software package that is designed to calculate three dimensional, unsteady and reacting flow-fields. FLUENT uses finite element methods on an unstructured mesh to solve the conservation equations, including the conservation of species in the case of reacting flows. In the present study FLUENT is used to model the Bunsen type burner flow-field. The program setup and solution process for the Bunsen type burner model is described in this section.

The Bunsen burner CFD model for solution by FLUENT is set up for a 2-D, axisymmetric computational domain using the segregated solver. Once the boundary conditions are set (See Section 7.5.2), the flow-field for the non-reacting case is calculated, with all species conservation equations and all momentum conservation equations active. The energy conservation equation is not yet activated because it is not required to solve an isothermal flow-field. The next step is to add gravitational acceleration as a parameter of the problem. Setting the gravitational acceleration allows the calculation of buoyancy forces which are important in the Bunsen type burner. The energy equation is also activated at this point. To 'ignite' the mixture a region of cells is artificially assigned the temperature of 3000 °K. The region of cells chosen represents the cells where the mole-fraction of methane is between 0.005 and 0.01, after mixing with the co-flow of air. The relaxation factor for the now activated energy equation is set to 0.01.

The low relaxation factor allows the species profiles to develop relatively independently of the temperature updates. It is important to establish the species gradients together with the temperature gradient because both heat and species diffusion help stabilize the flame. Once the species profiles are established, the energy equation relaxation factor is increased to 0.3, but never beyond that level unless unsteady calculations are performed. About 3000-5000 iterations after the relaxation factor has been increased, the solution is converged. To check that a true steady state has been achieved, the CFD model setup is changed and unsteady calculations are performed.

In all cases studied a steady state was reached after 0.5 seconds using 0.01 second time-steps.

The Bunsen burner CFD solution is discussed in detail in Section 7.5. For more information on solution processes employed by Fluent, the reader is referred to the Fluent User Manual (Fluent Inc., 1998).